

LASER ACCELERATION IN VACUUM

J.L. Hsu, T. Katsouleas

University of Southern California, Los Angeles, CA 90089-0484

W.B. Mori

University of California, Los Angeles, CA 90024

C. B. Schroeder, J.S. Wurtele

Lawrence Berkeley National Laboratory, Berkeley, CA 94720

Abstract

This paper explores the use of the large electric fields of high-brightness lasers (e.g., up to order TV/cm) to accelerate particles. Unfortunately, as is well known, it is difficult to couple the vacuum field of the laser to particles so as to achieve a net energy gain. In principle, the energy gain near the focus of the laser can be quite high, i.e., on the order of the work done in crossing the focus $\Delta\gamma = \sqrt{\pi eEW} \sim 30 \text{ MeV} \sqrt{P/1\text{TW}}$, where P is the laser power. In order to retain this energy, the particles must be in the highly nonlinear regime ($V_{osc}/c \gg 1$) or must be separated from the laser within a distance on the order of a Rayleigh length from the focus. In this work, we explore the acceleration and output energy distribution of an electron beam injected at various angles and injection energies into a focused laser beam. Insight into the physical mechanism of energy gain is obtained by separating the contributions from the longitudinal and transverse laser field components.

I. INTRODUCTION

The rapid development of high-brightness lasers leads us to re-examine the interaction of electron beams with vacuum focused lasers. For example, PetaWatt $1\mu\text{m}$ lasers are nearly available. For such lasers, the electric fields at focus will approach a TV/cm. There has been considerable previous work on this topic, so the limitations to energy gain via a linear interaction are by now well known¹. This paper is concerned with the highly non-linear regime (normalized quiver velocity $eE/m\omega c \gg 1$) where a net energy gain is possible. Here, we present preliminary numerical results of the net energy gain, energy spread and angular spread that may be expected by injecting an electron beam at various angles into a focused PetaWatt-class laser. The goal of the simulation is to determine the net work done on a relativistic electron as it propagates through a laser focal zone. Insight into the physical mechanism responsible for the energy gain is obtained by separating the contribution from the longitudinal and transverse field components.

II. ALGORITHM

For a linearly polarized, cylindrically focused Gaussian

beam propagating in the +z direction, the field (for y=0) components are²

$$\begin{aligned} E_x &= E_0 \frac{w_0}{w} \exp\left(-\frac{r^2}{w^2}\right) \cos\phi \\ E_z &= 2E_0 \frac{w_0}{w} \frac{x}{kw^2} \exp\left(-\frac{r^2}{w^2}\right) \left(\sin\phi - \frac{z}{z_0} \cos\phi\right) \\ B_y &= E_x \end{aligned} \quad (1)$$

with the phase

$$\phi = kz - \omega t + \frac{z^2}{w^2 z_0} - \tan^{-1}(z/z_0) \quad (2)$$

where w_0 is the spot size, w is the laser field radius at position z , $z_0 = \pi w_0^2 / \lambda$ is the Rayleigh length, and k is the free-space wave number of the laser.

The numerical algorithm is straightforward. Given the initial velocity of this particle, then the EM force can push this electron into a new position with a new velocity after a small time step by using the Time Center Leap Frog method³.

The maximum energy gain from the acceleration⁴ can be evaluated and compared to analytic estimates. The approximate value is given by estimating maximum work done by the laser field when the electron crosses the laser beam:

$$\begin{aligned} \Delta\gamma^{\text{max}} &\approx \int_{-w}^{+w} \vec{E} \cdot d\vec{r} \\ &\approx \sqrt{\pi} \cdot w_0 \cdot E_{\perp} + \int E_z dz \\ &\approx 30M \text{ eV} \sqrt{P/1\text{TW}} \end{aligned} \quad (3)$$

where P is the laser power in units of TW. For example, if we have a 100 TW laser, then the maximum energy gain is no more than 300MeV. In the following section, we use the model just described to analyze three specific laser acceleration geometries: one is injecting electrons at a small incident angle; the second is coaxial injection; and the third is injecting down the axis of the two crossed laser beams.

III. SIMULATION RESULTS

1. Small Incident Angle Injection:

In Fig.1, the x-z plot shows a laser beam propagating from $z = -72000 \mu\text{m}$ to $z = +72000 \mu\text{m}$ in the z direction.

An electron is injected from the left bottom corner where $z = -72000 \mu\text{m}$ crossing the laser beam with a small incident angle θ . For the parameters used in the example: the laser wavelength λ is $10.6 \mu\text{m}$, which corresponds to a CO_2 laser, in order to compare to parameters of UCLA CO_2 laser experiment. The laser waist width w is $200 \mu\text{m}$; the normalized laser amplitude, $eE_0/m\omega c \equiv aa$, is 0.4 ; the initial electron energy γ is 32 ; and the electron incident angle θ is 0.04 rad. The energy of the electron γ is plotted versus the propagating direction z from $-72000 \mu\text{m}$ to $+72000 \mu\text{m}$ and shown in the bottom side. We can see from the γ - z plot that γ increases and decreases as the particle slips in phase behind the light wave, finally reaching the same value as its initial energy. In this example, aa is not large enough to induce nonlinear effects, so no net energy gain results, as expected from the Lawson-Woodward theorem¹.

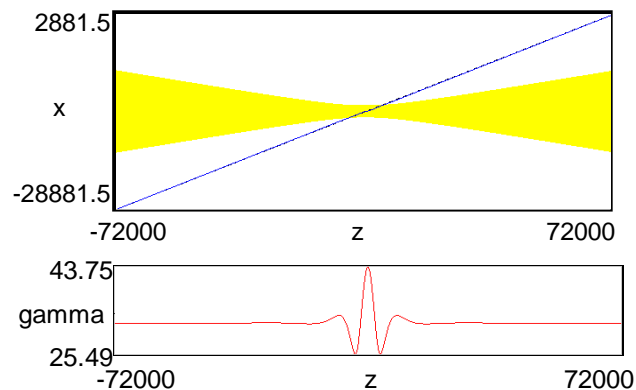


FIGURE 1. Particle trajectory and (below) particle energy (γ) vs. z for $aa=0.4$.

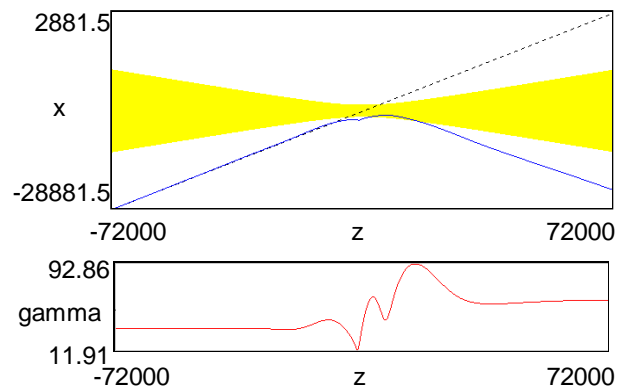


FIGURE 2. Particle trajectory and (below) particle energy gain vs. z for $aa = 4$. γ increase from 32 to 59.4 (dotted line shows the incident direction for this electron).

In the second example (Fig. 2), we increase aa from 0.4 to 4 , which means that the laser power is 100 times that of the first one. From the (lower) γ - z plot in Fig. 2, we see that there is a net increase in the energy γ due to

the interaction. The final energy at the point $z = 72000 \mu\text{m}$ depends on the initial phase of the electron injection into the laser fields. In this example, the maximum $\Delta\gamma$ in a particular initial laser phase is near 27.4 ; that is 5% of the maximum value we estimated using the work done by the laser in equation (3).

2. Coaxial Injection:

Before considering the coaxial injection into focused laser beams, consider the movement of electrons in infinite plane waves. The exact solution for an electron moving in an infinite plane wave can be expressed as a drifting “figure eight”. Using a large beam waist w in our simulation program approximates the plane wave limit; the trajectory of an electron in Fig.3 exhibits similar behavior to the exact solution in an infinite plane wave.

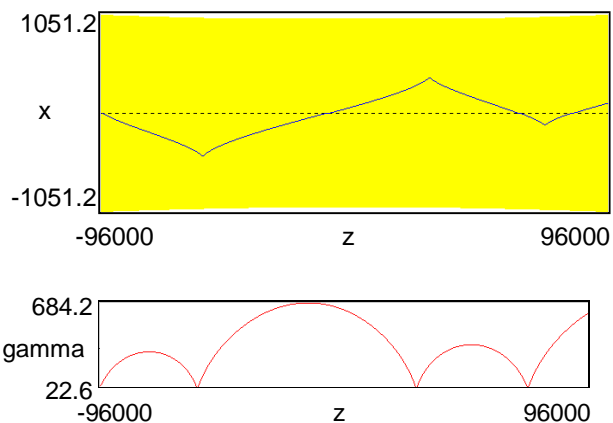


FIGURE 3. Particle trajectory and (below) γ - z plot for coaxial injection with large laser waist.

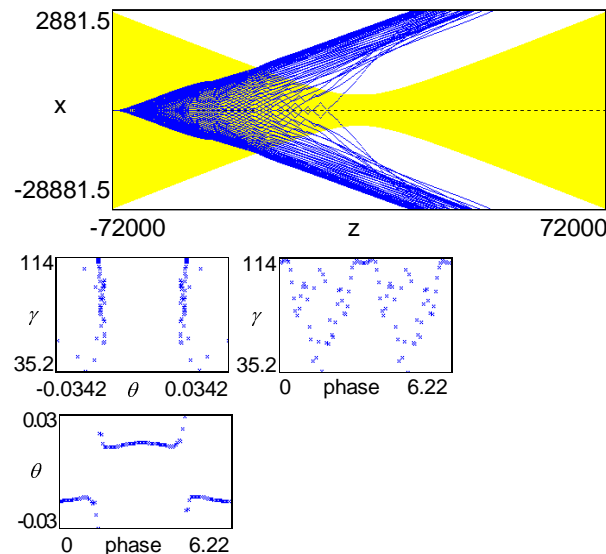


FIGURE 4. Particle trajectories for 100 initial laser phases from 0 to 2π and insets: final γ vs. initial laser phase, final γ vs. outgoing angle θ , θ vs. initial laser phase.

When the laser beam is focused to small spot size w , the trajectories of coaxially injected electrons are quite different. The trajectories of coaxially injected electrons with initial laser phases distributed from 0 to 2π are shown in Fig.4. The initial energy for the electrons is $\gamma=32$, and the γ - θ plot (the first inset) shows the final γ measured at the point $z = 72000 \mu\text{m}$ versus different outgoing angle θ . As the second inset (γ -phase plot) shows, at the injection phases of 0 and π the final energy is relatively insensitive to injection phases (over approximately 1.7 radians or 27% of the full laser wavelength). Therefore, particle injection at these phases will result in better output beam quality (i.e., small energy spread and emittance growth). By Comparison the runs we have done with injection at a small angle, were very sensitive to the injection phase.

Based on the results of Fig.4, it appears that a 100TW laser could be used to accelerate a micro-bunch ($1.4 \mu\text{m}$ or 14% of the bucket) of cold electrons from 16MeV to 26MeV with an energy spread of 0.4MeV and emittance growth of $\varepsilon_x \approx 1\text{mm-mrad}$. The maximum energy gain in this example is only 3.8% of the maximum value from equation (3). By raising γ to 64 (not shown), we could increase the energy gain to 9.1%, but the particles with highest energy were from a very small region of initial phases (2% of the bucket).

In order to separate the effects of transverse and longitudinal fields in the acceleration process, we turn off the longitudinal field and find the interaction with the transverse field only. We observe that the electron trajectories are considerably altered by the presence of the E_z field, even though we found that the $\int E_z dz$ contribution to net energy gain was much smaller than the $\int E_\perp dy$ term for our examples.

3. Crossed Beam Injection:

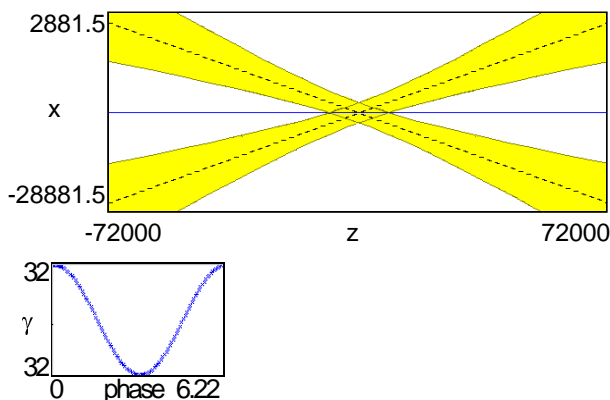


FIGURE 5. Numerical simulation showing no energy gain for any injection phase in two crossed lasers (dotted lines show laser beam axes).

A laser geometry that has received attention is the case of two gaussian laser beams crossed at a small angle with respect to the axis of electron injection^{5,6}. The advantage of this geometry is that the transverse electric and magnetic fields will cancel on axis, leaving only the axial electric field to accelerate the particles. Fig.5 shows the simulation results of electrons injected at various initial laser phases on axis into the crossed beams which are positioned at an angle of 0.04 rads with respect to the electron beam. As the inset shows, there was no net energy gain for any initial laser phases. This result can be explained by realizing that by arranging the geometry such that there is only an electric field along the direction of motion, we have eliminated the nonlinear forces which are necessary for laser acceleration in vacuum. This is consistent with the results of P. Sprangle et al.⁷

IV. CONCLUSION

The simulation results show that net energy gain can be extracted from a single laser via nonlinear interactions. The nonlinear energy gain comes from the transverse fields; while the longitudinal field affects the path of electrons but does not increase their energy gain. If initial injection energy and angle and laser amplitude are chosen properly, large scattering spread angle can be avoided. For further research, characteristics of the outgoing electron beam with respect to the injected beam emittance need to be investigated. Other acceleration schemes, such as axicon focused lasers⁵, or standing wave acceleration in two counterpropagating lasers⁸ are also of interest for further simulations with this code.

V. ACKNOWLEDGMENTS

Work supported by US Department of Energy DOE - AC#DE - FG03 - 92ER40745. The assistance of R. Kinter and D.Gordon in coding the numerical model is gratefully acknowledged.

VI. REFERENCES

- [1] P.M. Woodward, *JIEE* 93, 1947, p.1554.
- [2] R. Guenther, *Modern Optics*, (Wiley, New York 1990), p.336.
- [3] C.K. Birdsall and A.B. Langdon, *Plasma Physics via Computer Simulation*, (McGraw-Hill, NY 1985).
- [4] W. Mori and T. Katsouleas, in *Advanced Accelerator Concepts*. AIP Conf. Proc. No. 335, (AIP, NY 1994), p.112.
- [5] L. Steinhauer et al, in *Advanced Accelerator Concepts*, AIP Conf. Proc. No. 335, (AIP, NY 1994), p.131.
- [6] C. M. Haaland, *Optics Comm.* 114, 280 (1995).
- [7] P. Sprangle, *Optics Comm.* 124, 69 (1996).
- [8] C. Barty, private communication.